

Biomedical Electronic Devices

Capacitive Micromachined Ultrasonic Transducer	----- 59
Fluorescence Immunochromatographic Assay Strip Readers	----- 60
Galvanic Coupling Intrabody Communication	----- 61
A Handheld High-Sensitivity Micro-NMR CMOS Platform with B-Field Stabilization for Multi-Type Biological/Chemical Assays	----- 62
Portable NMR with Parallelism	----- 63
An Integrated Circuit for Simultaneous Optogenetic Neural Manipulation and Electrophysiology Recording with Programmable 300mA LED/Laser Drivability	----- 64
Brain Rhythm Sequencing Using EEG Signals:A Case Study on Seizure Detection	----- 66
Low-latency single channel real-time neural spike sorting system based on template matching	----- 68

Capacitive Micromachined Ultrasonic Transducer

Sio Hang Pun and Mang I Vai

FOCUS ON

Analytical Modeling
High Frequency CMUT Design

POTENTIAL APPLICATIONS

Medical Imaging
Underwater Imaging

DESCRIPTION

Analytical modeling of CMUT is one of the commonly used modeling methods and has the advantages of intuitive understanding of the physics of CMUTs and convergent when modeling of collapse mode CMUT. Modeling of the membrane deflections are characterized by governing equations from Timoshenko, von Kármán equations and the 2D plate equation, and solved by various methods such as Galerkin's method and perturbation method. Analytical expressions from Timoshenko's equation can be used for small deflections, while analytical

expression from von Kármán equations can be used for both small and large deflections. Building the model can be very helpful for understanding and designing CMUT with different requirements.

An embossed capacitive micromachined ultrasonic transducer (CMUT) is a device with embossed membrane that works in the collapse mode to improve output pressure in transmission. With the help from the modeling, a six-mask sacrificial release process is proposed for fabricating embossed CMUT arrays. Based on this process, the embossed pattern CMUTs were firstly fabricated. By using of electroplating methods, annular embossed patterns made of nickel were grown on the full top electrodes of CMUTs. The dimensions of the embossed pattern were about $3.0\text{ }\mu\text{m}$ in width and $1.4\text{ }\mu\text{m}$ in height. The resonant frequencies of the embossed CMUT array were 6.4MHz and 8.7MHz when the device worked in the conventional and the collapse mode, respectively.

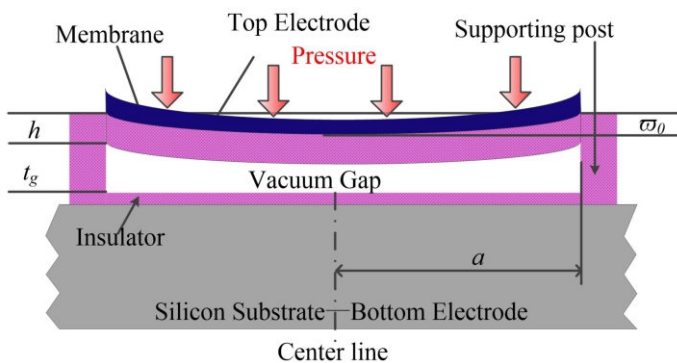


Fig. 1. The cross-sectional view of a collapse CMUT with full top electrode

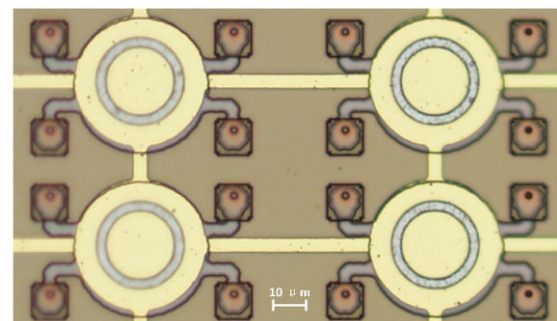


Fig. 2. Embossed CMUTs observed by an optical microscope

Publication(s)

- [1] J Wang, X Liu, Y Yu, Y Li, C Cheng, S Zhang, P Mak, M Vai, S Pun, "A Review on Analytical Modeling for Collapse Mode Capacitive Micromachined Ultrasonic Transducer of the Collapse Voltage and the Static Membrane Deflections," *Micromachines*, vol. 12, no. 6, pp. 714, Jul 2021.
- [2] Y Yu, J Wang, S Pun, C Cheng, K Lei, M Vai, S Zhang, P Mak, "Fabrication of embossed capacitive micromachined ultrasonic transducers using sacrificial release process," *IEICE Electronics Express*, vol 16, no 2, pp. 20181002-20181002, 2019

Sponsorship

National Natural Science Foundation of China, Chinese Ministry of Science and Technology, S&T Department of Fujian Province, FDCT, University of Macau

Fluorescence Immunochromatographic Assay Strip Readers

Sio Hang Pun and Mang I Vai

FEATURES

Detection range, 1-1024 $\mu\text{g/mL}$

Goodness of fit > 0.99

DESCRIPTION

Fluorescence immunochromatographic assay (FICA) is a quantitative detection technique widely used in clinical diagnosis, environmental monitoring, and food safety. To deal with the limited applications caused by insufficient detection range, a photoelectric adjustment system suitable for FICA strip readers to expand its detection was developed.

This photoelectric adjustment system is proposed based on the relationship between the excitation

light intensity and the fluorescence intensity, which provides the optimal excitation light intensity and a stable baseline amplitude for the FICA strip reader.

The system was applied to the strip reader previously developed. The results show that the linear detection range of the FICA strip reader was extended from 1.95-256 $\mu\text{g/mL}$ to 1-1024 $\mu\text{g/mL}$. At the same time, the accuracy of the FICA strip reader does not deteriorate and is in good comparisons with the conventional ESEQuant Lateral Flow Reader (with $R^2 > 0.9987$). The proposed photoelectric adjustment method and system can improve the detection range of the strip reader or other similar devices.

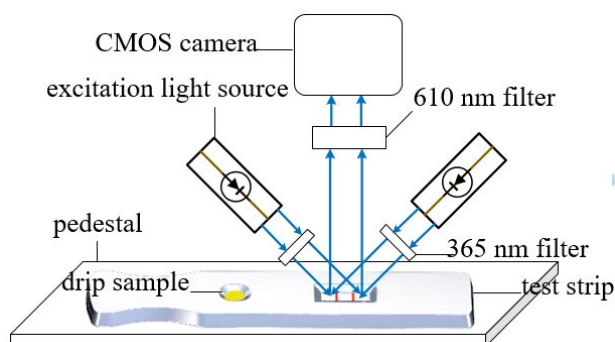


Fig. 1. Image acquisition device of the fluorescence immunochromatographic assay (FICA) reader based on image processing.

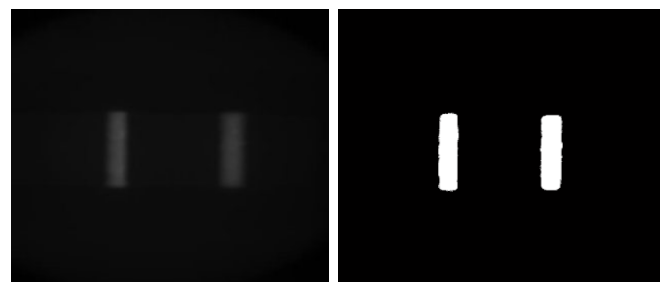


Fig. 2. 5. Results of image segmentation: left: original image; right: segmented image

Publication(s)

- [1] H. Wu, Y. Gao, J. Yang, M. Vai, M. Du and S. Pun, "Development of a Photoelectric Adjustment System With Extended Range for Fluorescence Immunochromatographic Assay Strip Readers," in IEEE Photonics Journal, vol. 13, no. 3, pp. 1-12, June 2021, Art no. 6600512.
- [2] Jiang R, Wu H, Yang J, Jiang H, Du M, Vai M, Pun S, Gao Y, "Automatic Range Adjustment of the Fluorescence Immunochromatographic Assay Based on Image Processing", Sensors, 20(1):209, Dec. 2019.

Sponsorship

Chinese Ministry of Science and Technology, National Natural Science Foundation of China, Fujian Provincial Department of Science and Technology

Galvanic Coupling Intrabody Communication

Sio Hang Pun and Mang I Vai

POTENTIAL APPLICATIONS

In-Vivo Networking

Leadless Cardiac Pacemaker

DESCRIPTION

Galvanic coupling intrabody communication (IBC) is a low-power, low-cost wireless communication scheme that utilizes the human body as a medium to develop a body area network in IEEE 802.15.6.

Intrabody communication (IBC) can achieve better power efficiency and higher levels of security than other traditional wireless communication technologies. The existing IBC studies mainly focus on human channel characteristics of the physical layer, transceiver design for the application, and the protocol design for the networks. The human channel model used in most of the studies is just a multi-layer homocentric cylinder model.

Besides these, the majority of research on the body channel characteristics of galvanic coupling IBC are motionless and have only been evaluated in the frequency domain. Given

the long measuring times of traditional methods, the access to dynamic variations and the simultaneous evaluation of the time-frequency domain remains a challenge for dynamic body channels such as the cardiac channel.

Our research tried to propose methods to accurately approximate the real human tissue layer and capturing dynamic variations in the body channel and provides a more comprehensive evaluation and richer information for the study of IBC.

To address this challenge, we proposed a parallel measurement methodology with a multi-tone strategy and a time-parameter processing approach to obtain a time-frequency evaluation for dynamic body channels. A group search algorithm has been performed to optimize the crest factor of multitone excitation in the time domain. To validate the proposed methods, in vivo experiments, with both dynamic and motionless conditions were measured using the traditional method and the proposed method. Most importantly, it is capable of capturing dynamic variations in the body channel and provides a more comprehensive evaluation and richer information for the study of IBC.

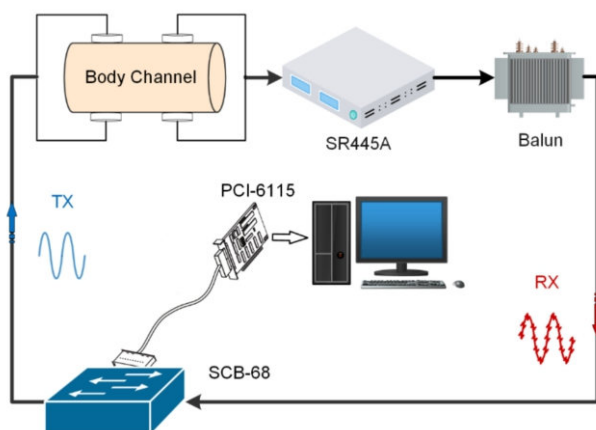


Fig. 1. Schematic diagram of experimental platform construction.

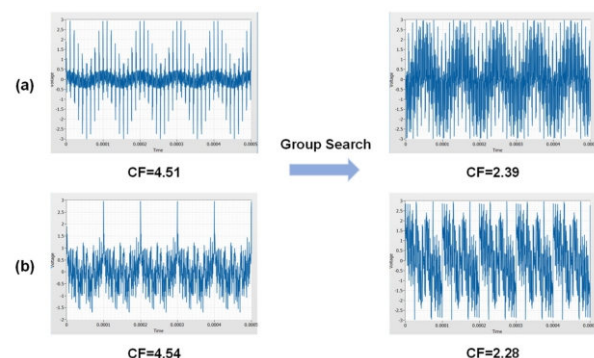


Fig. 2. The time domain waveform and its crest factors (CF) of the multitone before and after group search algorithm. (a) denotes linearly distributed multitone and (b) denotes quasi-logarithmically distributed multitone.

Publication(s)

- [1] Z Wei, Y Wen, Y Gao, M Yang, J Yang, S Pun, M Vai, M Du, "A Time-Frequency Measurement and Evaluation Approach for Body Channel Characteristics in Galvanic Coupling Intrabody Communication," *Sensors*, vol. 21, no. 2, pp 348, Jan 2021
- [2] Y Gao, Hi Zhang, S Lin, R Jiang, Z Chen, Ž Vasić, M Vai, M Du, M Cifrek, S Pun, "Electrical exposure analysis of galvanic-coupled intra-body communication based on the empirical arm models," *Biomedical engineering online*, vol. 17, no1, pp. 1-16, Dec 2018

Sponsorship

National Natural Science Foundation of China, Chinese Ministry of Science and Technology, S&T Department of Fujian Province, FDCT, University of Macau

A Handheld High-Sensitivity Micro-NMR CMOS Platform with B-Field Stabilization for Multi-Type Biological/Chemical Assays

Ka-Meng Lei, Hadi Heidari, Pui-In Mak, Man-Kay Law, F. Maloberti and R. P. Martins

FEATURES

First micro-NMR CMOS platform apt for multi-type biological/chemical assays

Low sample consumption (120× less)

Lightweight size (96× smaller and 175× smaller)

DESCRIPTION

We report a micro-nuclear magnetic resonance (NMR) system compatible with multi-type biological/chemical lab-on-a-chip assays. Unified in a handheld scale (dimension: $14 \times 6 \times 11 \text{ cm}^3$, weight: 1.4 kg), the system is capable to detect $<100 \text{ pM}$ of *Enterococcus faecalis* derived DNA from a $2.5 \mu\text{L}$ sample.

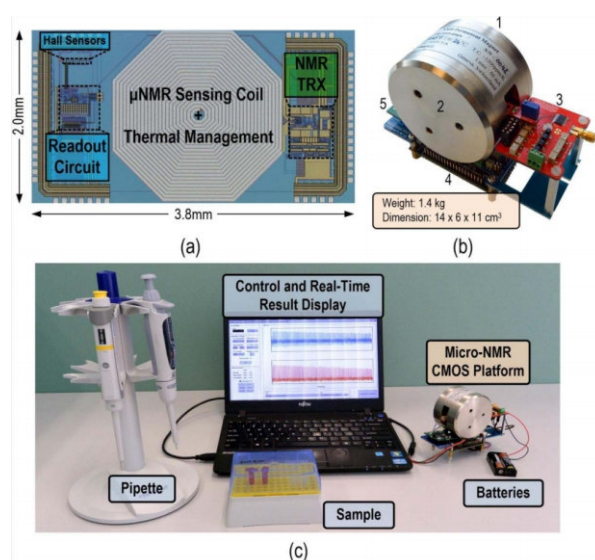


Fig. 1. (a) Chip photograph. (b) Prototype of the micro-NMR platform, including: 1) permanent magnet; 2) CMOS micro-NMR chip (inside magnet); 3) PCB; 4) FPGA and 5) current driver. (c) Experimental setup.

The key components are a portable magnet (0.46 T, 1.25 kg) for nucleus magnetization, a system PCB for I/O interface, an FPGA for system control, a current driver for trimming the magnetic (B) field, and a silicon chip fabricated in $0.18 \mu\text{m}$ CMOS. The latter, integrated with a current-mode vertical Hall sensor and a low-noise readout circuit, facilitates closed-loop B-field stabilization ($2 \text{ mT} \rightarrow 0.15 \text{ mT}$), which otherwise fluctuates with temperature or sample displacement. Together with a dynamic-B-field transceiver with a planar coil for micro-NMR assay and thermal control, the system demonstrates: 1) selective biological target pinpointing; 2) protein state analysis; and 3) solvent-polymer dynamics, suitable for healthcare, food and colloidal applications, respectively. Compared to a commercial NMR-assay product (Bruker mq-20), this platform greatly reduces the sample consumption (120×), hardware volume (175×), and weight (96×).

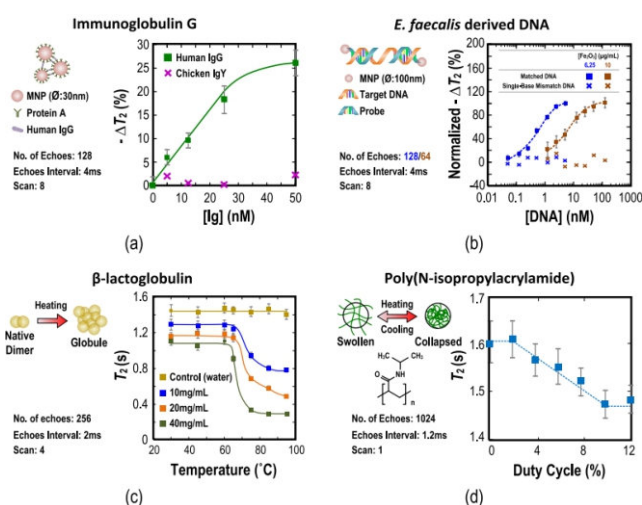


Fig. 2. Experimental results from biological/chemical samples. (a) Target quantification from human IgG as target and chicken IgY as control. (b) Target quantification from *Enterococcus faecalis* derived DNA together with single-base mismatch DNA. (c) Protein (β -LG) state detection with different heating temperature. (d) Polymer (PNIPAM) dynamics with the solvent during heating from the on-chip heater.

Publication(s)

- [1] K.-M. Lei, H. Heidari, P.-I. Mak, M.-K. Law, F. Maloberti, and R. P. Martins, "A Handheld High-Sensitivity Micro-NMR CMOS Platform with B-Field Stabilization for Multi-Type Biological/Chemical Assays," *IEEE Journal of Solid-State Circuits*, vol. 52, pp. 284-297, Jan. 2017.
- [2] K.-M. Lei, H. Heidari, P.-I. Mak, M.-K. Law, R.P. Martins, and F. Maloberti, "A handheld 50pM-sensitivity micro-NMR CMOS platform with B-field stabilization for multi-type biological/chemical assays," in *IEEE Int. Solid-State Circuits Conf. (ISSCC) Dig. Tech. Papers*, pp. 474-475, Feb. 2016

Sponsorship

Macau Science and Technology Development Fund (FDCT), Research Committee of University of Macau.

Portable NMR with Parallelism

Ka Meng Lei, Dongwan Ha, Yi-Qiao Song, Robert Westervelt, Rui Martins, Pui-In Mak, and Donhee Ham

FEATURES

Portable NMR system featuring customized CMOS IC

Parallelized operation, reducing the overall experiments time

Shim coil to enhance the homogeneity and resolution

DESCRIPTION

Portable NMR combining a permanent magnet and a complementary metal-oxide-semiconductor (CMOS) integrated circuit has recently emerged to offer the long desired online, on-demand, or in situ NMR analysis of small molecules for chemistry and biology.

Here we take this cutting-edge technology to the next level by introducing parallelism to a state-of-the-art portable NMR platform to accelerate its experimental throughput, where NMR is notorious for inherently low throughput. With multiple (N) samples inside a single magnet, we perform simultaneous NMR analyses using a single silicon electronic chip, going beyond the traditional single-sample-per-magnet paradigm. We execute the parallel analyses via either time-interleaving or magnetic resonance imaging (MRI). In

the time-interleaving method, the N samples occupy N separate NMR coils: we connect these N NMR coils to the single silicon chip one after another and repeat these sequential NMR scans. This time-interleaving is an effective parallelization, given a long recovery time of a single NMR scan.

To demonstrate this time-interleaved parallelism, we use $N = 2$ for high-resolution multidimensional spectroscopy such as J-coupling resolved free induction decay spectroscopy and correlation spectroscopy (COSY) with the field homogeneity carefully optimized (<0.16 ppm) and $N = 4$ for multidimensional relaxometry such as diffusion-edited T_2 mapping and T_1 - T_2 correlation mapping, expediting the throughput by 2–4 times. In the MRI technique, the N samples ($N = 18$ in our demonstration) share 1 NMR coil connected to the single silicon chip and are imaged all at once multiple times, which reveals the relaxation time of all N samples simultaneously. This imaging-based approach accelerates the relaxation time measurement by 4.5 times, and it could be by 18 times if the signal-to-noise were not limited. Overall, this work demonstrates the first portable high-resolution multidimensional NMR with throughput-accelerating parallelism.

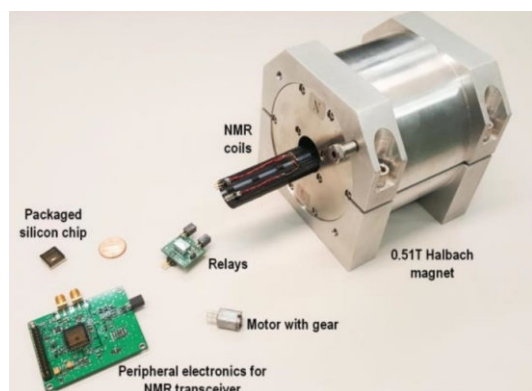


Fig. 1. Portable NMR with parallelism. Our portable NMR platform, whose key components are the Halbach magnet and the silicon IC we developed.

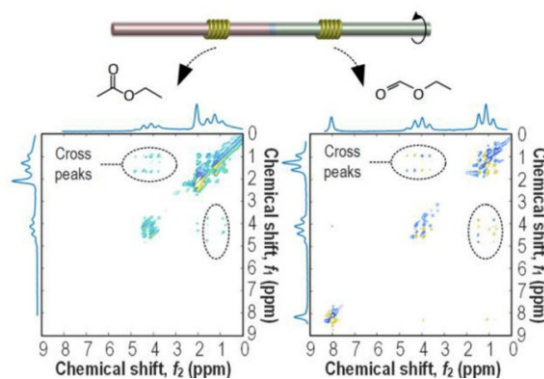


Fig. 2 Measured 2D ¹H NMR spectra with time-interleaving (2 NMR samples with 2 coils) from ethyl formate and ethyl acetate. Each sample undergoes 404 total scans.

Publication(s)

[1] Ka Meng Lei, Dongwan Ha, Yi-Qiao Song, Robert Westervelt, Rui Martins, Pui-In Mak, and Donhee Ham, "Portable NMR with Parallelism," ACS Analytical Chemistry, 2020, 92, 2, 2112-2120.

Sponsorship

Macau Science and Technology Development Fund (FDCT).

An Integrated Circuit for Simultaneous Optogenetic Neural Manipulation and Electrophysiology Recording with Programmable 300mA LED/Laser Drivability

Chang Hao Chen, Elizabeth A McCullagh, Sio Hang Pun, Peng Un Mak, Mang I Vai, Mak Pui In , Achim Klug, Tim C. Lei

FEATURES

Optogenetic chip

low input capacitance of 9.7 pF

low input referred noise 4.57 μVrms

high driving current of 330 mA

DESCRIPTION

ELECTROPHYSIOLOGICAL recordings of action potentials in the brain have been one of the most important research tools available for neuroscientists to decipher the function of neuronal circuits. In addition to recording naturally occurring neuronal activity and to gain further insights into functions of these circuits, many neuroscientists desire to manipulate neuronal activity experimentally. One such method is the manipulation of neuronal circuits with light (optogenetics) to control complex neuronal functions, including behavior.

Several studies have been published regarding neural acquisition amplifier designs. However, most of these studies were focused on the ability to record from multiple electrodes, reduce power consumption, and improve the noise efficiency factor. The role of the amplifier's input impedance, which is one of the important parameters for extracellular recordings, has not received much attention in these designs. Tailoring the input impedances of amplifiers allows for selective measurements of local field potentials, action potentials from multiple neurons, or action potentials from a single neuron. In particular, a high impedance electrode with a small recording surface is necessary to record single neuronal activity and designs of neural amplifiers specially tailored for this application are relatively few.

We developed a monolithic IC that integrates a low-noise neural amplifier for action potential recording and a high current laser/LED driver for simultaneous optogenetic control to help meet the needs of this new and important trend of using optogenetics in neuroscience. In addition, an electrical noise model for the recording amplifier was derived to guide the amplifier design. In the model, noise sources from both the high impedance metal electrode and the optogenetic control process were included. The performance of the IC was tested with anesthetized Mongolian gerbils from which action potentials were recorded from the inferior colliculus in the midbrain. Additionally, we were able to inhibit spontaneous neural firings of the fifth nerve using optogenetics and an implantable "optrode" that includes a high input impedance electrode and the optical illumination fiber. Our results indicated that an integrated laser/LED controller can deliver a maximum current of 330 mA, which is adequate to effectively drive a laser to inhibit neural activity in the brainstem. The recording amplifier has a low input capacitance of 9.7 pF optimized for the use of high impedance electrodes for single cell extracellular recording. The input referred noise of the amplifier was measured to be 4.57 μVrms and the recorded action potentials had a signal-to-noise ratio of at least 6.6. Therefore, we believe that the use of this multi-functional IC system may reduce the complexities of using optogenetics with electrophysiology recording for current and future in-vivo and behavioral experiments to test various hypotheses in neuroscience.

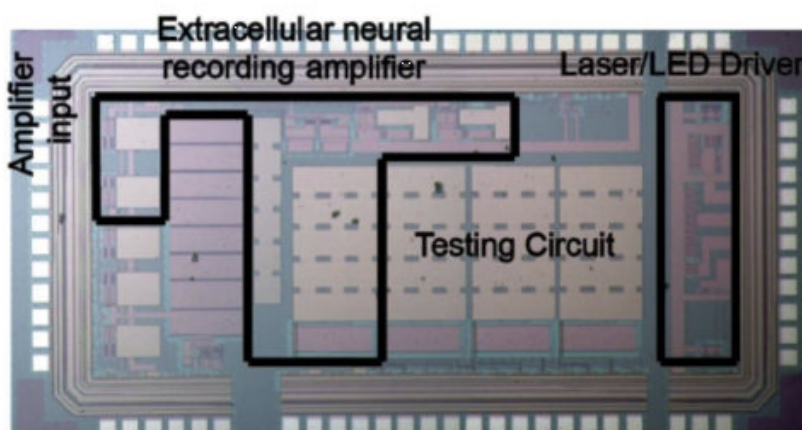


Figure A photograph of the fabricated IC with dimension of 2.9 mm \times 1.6 mm. The actual neural amplifier and the laser/LED driver unit occupies about half of the space, with the rest of the space occupied by additional testing circuits.

Continuous 

An Integrated Circuit for Simultaneous Optogenetic Neural Manipulation and Electrophysiology Recording with Programmable 300mA LED/Laser Drivability

Chang Hao Chen, Elizabeth A McCullagh, Sio Hang Pun, Peng Un Mak, Mang I Vai, Mak Pui In , Achim Klug, Tim C. Lei

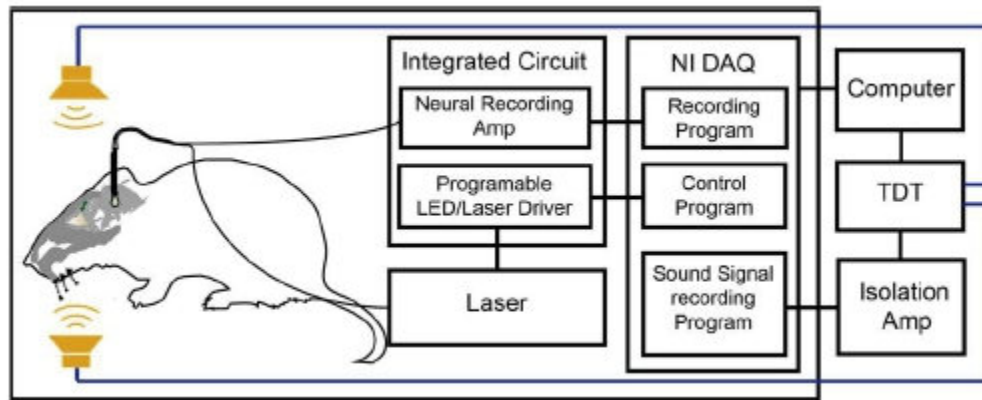


Figure 2 Experimental setup for simultaneous optogenetic inhibition and electrophysiological recordings from the brainstem of an anesthetized gerbil. The IC was connected to a data acquisition card (NI-DAQ) for signal digitization and laser power control. An isolation amplifier was used to isolate the neural amplifier from environmental noise. An audio signal processor (TDT) was used to generate a tonal signal to drive two speakers placed in the ears of the gerbil for auditory stimulation of the inferior colliculus.

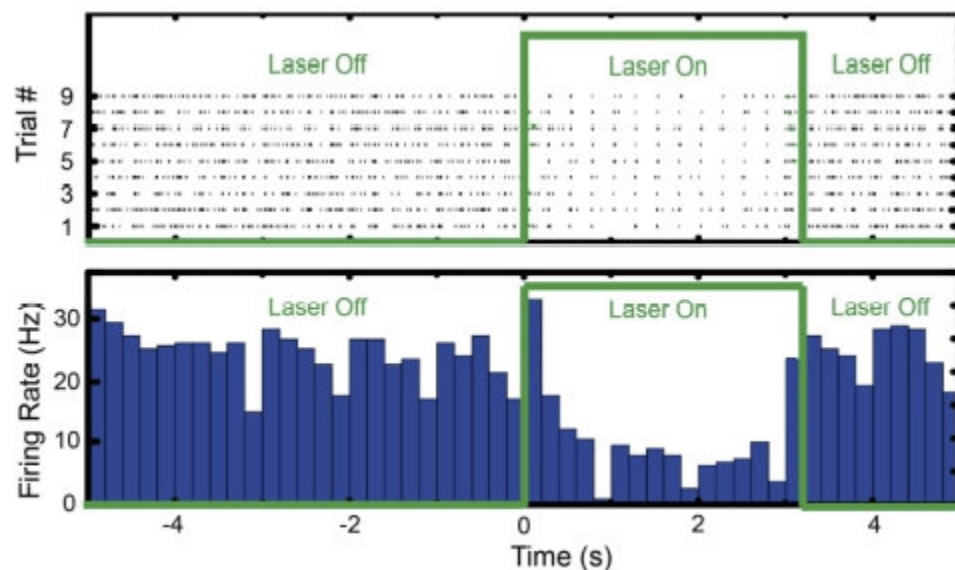


Figure 3 (A) Raster plot showing the temporal locations of action potential firing over nine optogenetic inhibition trials. (B) The calculated average firing rate showing significant reduction of the firing rate during optical illumination.

Publication(s)

Chen CH, McCullagh EA, Pun SH, et al. An Integrated Circuit for Simultaneous Extracellular Electrophysiology Recording and Optogenetic Neural Manipulation. IEEE Trans Biomed Eng. 2017;64(3):557-568. doi:10.1109/TBME.2016.2609412

Sponsorship

Macau Science and Technology Development Fund (FDCT), Research Committee of University of Macau.

Brain Rhythm Sequencing Using EEG Signals: A Case Study on Seizure Detection

Jia Wen Li, Shovan Barma, Peng Un Mak, Sio Hang Pun, and Mang I Vai

FEATURES

Low-latency real time neural spike sorting system
maximal spike sorting rate of 941 spikes/second
sorting latency less than 2 ms

DESCRIPTION

Brain rhythms are one series of trustworthy patterns that have been commonly employed for EEG-based applications. Moreover, they are generated from the classifications of EEG signals based on the five specific sub-bands: delta (δ , 0–4 Hz), theta (θ , 4–8 Hz), alpha (α , 8–13 Hz), beta (β , 13–30 Hz), and gamma (γ , 30–50 Hz). In fact, the effect of the brain rhythms is that the presence or change of certain brain rhythms can be considered as clues to recognize and detect mental diseases, neurological disorders, and affective reactions. For instance, the changes in α power can significantly indicate sleep disorders. In Alzheimer's disease (AD), compared with the healthy subjects, the indications of amplitude increase in δ and θ sources, and the amplitude decrease in α and/or β sources can be detected in the patients. As for affective reactions, the changes of power in γ are usually related to happiness and sadness, α power varied with the level of valence, and so on. Categorically, the brain rhythms are deliberated as the fundamental or key components in the frequency domain representations of EEG signals. However, the rhythmic time behaviors, i.e., the indications and consecutive existences of the brain rhythms, which are useful information to interpret the EEG with great details, have not been investigated yet.

To study such chronological orders of the brain rhythms, the particular one which is appropriate to distinguish the specific brain state can be identified so that the details about the time-related transformations between different brain states can be determined. Meanwhile, the characteristics of the particular rhythm patterns are also useful for investigating the effect of subject-dependent in a specific brain state. On the other hand, based on the similarity measurement of the rhythm patterns among different channels, the signals synchrony in terms of rhythms synchronization can be indicated, which provides a solution to decrease the number of applied channels by mean of selecting several representatives. Thereby, to focus on the properties of the brain rhythms in their corresponding times of occurrences could extend the analysis and characterization of EEG signals in a new way. Then, inspired by the sequence analysis in bioinformatics, a technique named brain rhythm sequencing which interprets and characterizes the EEG as the sequence data consisted of the five specific brain rhythms has been proposed in this work. Moreover, this idea can be tested and employed for various EEG-based applications such as the detections of some neurological disorders.

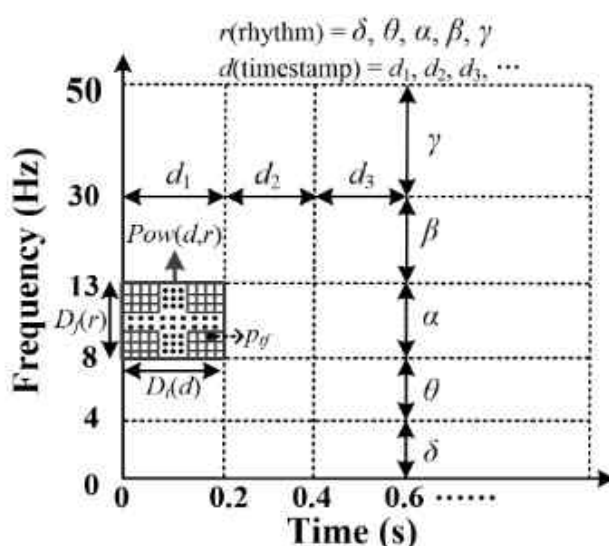


Figure 1 Power estimation of five brain rhythms at each timestamp by TFA (RSPWVD method); where r and d correspond to brain rhythm and time stamp respectively ; $Pow(d,r)$ presents the power value of one specific rhythm at a certain timestamp; ptf indicates the instantaneous power in each bound of the time-frequency plane; $Dt(d)$ and Df^* is the distance between adjacent timestamps and brain rhythms separately

Continuous

Brain Rhythm Sequencing Using EEG Signals: A Case Study on Seizure Detection

Jia Wen Li, Shovan Barma, Peng Un Mak, Sio Hang Pun, and Mang I Vai

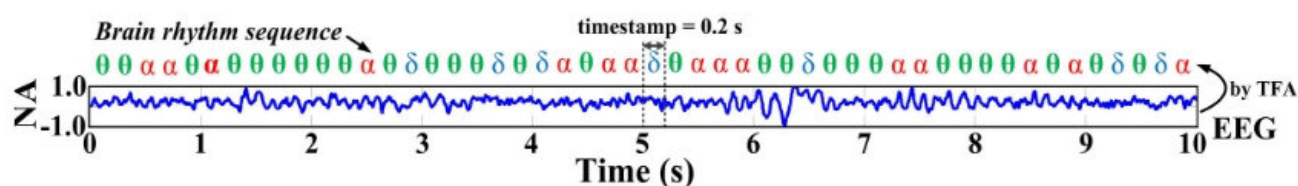


Figure 2 Brain rhythm sequencing from EEG signals based on choosing the prominent rhythm having the maximum power contribution at each timestamp of 0.2 s by TFA. Label: NA refers to normalized amplitude.

Channel	Coherence	Correlation	Mutual information	Rhythm sequencing
FP2	23.66%	21.51%	31.18%	24.73%
F4	84.95%	81.72%	82.80%	74.19%
C4	83.87%	80.65%	79.57%	73.12%
P4	60.22%	68.82%	63.44%	64.52%
F8	6.45%	13.98%	10.75%	12.90%
T4	66.67%	59.14%	52.69%	60.22%
T6	7.53%	11.83%	5.38%	8.60%
O2	4.30%	11.83%	6.45%	4.30%
FP1	2.15%	5.38%	9.68%	10.75%
F3	5.38%	1.08%	3.23%	7.53%
C3	8.60%	9.68%	3.23%	11.83%
P3	6.45%	2.15%	7.53%	9.68%
F7	0.00%	1.08%	1.08%	0.00%
T3	3.23%	6.45%	4.30%	7.53%
T5	0.00%	1.08%	4.30%	1.08%
O1	2.15%	0.00%	3.23%	1.08%

Figure 3 Results of representative channels based on proportions.

Publication(s)

J. W. Li, S. Barma, P. U. Mak, S. H. Pun and M. I. Vai, "Brain Rhythm Sequencing Using EEG Signals: A Case Study on Seizure Detection," in IEEE Access, vol. 7, pp. 160112-160124, 2019, doi: 10.1109/ACCESS.2019.2951376.

Sponsorship

Macau Science and Technology Development Fund (FDCT), Research Committee of University of Macau.

Low-latency single channel real-time neural spike sorting system based on template matching

Pan Ke Wang, Sio Hang Pun, Chang Hao Chen, Elizabeth A. McCullagh, Achim Klug,
Anan Li, Mang I. Vai, Peng Un Mak, Tim C. Lei

FEATURES

Low-latency real time neural spike sorting system
maximal spike sorting rate of 941 spikes/second
sorting latency less than 2 ms

DESCRIPTION

Recording action potentials from neurons in the brain gives neuroscientists the ability to study neural circuits with single cell accuracy. Typically neural spikes (or action potentials) are recorded extracellularly with a metal or glass electrode inserted into the brain of an animal or a human patient. By contrast, intracellular or patch clamp recordings with glass pipettes are much less common in vivo because pulsation, movement of brain tissue and electrode contamination make them very challenging. Therefore, electrodes are typically placed within the extracellular space between neurons to capture neural spikes extracellularly. In this extracellular configuration, neural spikes generated from several adjacent neurons are often captured by the electrode at the same time, hereafter referred to as multi-units, making it challenging to determine the activity patterns of single neurons included in the recording. These multi-unit recordings are especially common when signals are measured from brain areas densely packed with neurons. For this reason, spike sorting algorithms are often used off-line to separate the neural spikes and assign them to different cluster groups. The underlying principle of spike sorting relies on the fact that neural spikes originating from different neurons will have different temporal profiles. The temporal profiles of these neural spikes are dependent on the impedance of the extracellular fluid between the neurons and the electrode, the currents produced by each neuron, as well as the cell membrane area from which the ionic currents can reach the metal electrode.

There has been a sustained effort to develop better spike sorting algorithms aimed at increasing both the accuracy and the speed of the sorting process. From a mathematical perspective, spike sorting can be considered as an unsupervised classification problem, and several classification algorithms, including K-means, Expectation Maximization (EM) and Multivariate Gaussian Mixture, have been used to sort neural spikes. Besides these classification algorithms, superparamagnetic clustering (SPC) was specifically designed for neural spike sorting [9]. SPC borrows the physical concept of magnetic thermal interaction and models neural spikes as magnetic spin elements. As the temperature rises, the neural spin elements fracture into distinct groups for spike classification. Aksenova et al. modeled neural spikes as self-oscillating nonlinear oscillators and can be expressed by trajectories in the phase space described by a perturbed ordinary differential equation. Caro-Martin et al also extracted linear independent spike features based on shape, phase and distribution features for the spikes and sort neural spikes using the spike features based on a modified k-mean technique. The advantage of using phase space features instead of temporal shapes to sort neural spikes is less prone to amplitude fluctuation and non-Gaussian distributed cluster structures. In addition, there are several other off-line spike sorting algorithms that the clustering is based on consensus-based modified k-mean techniques, variational Bayes, and maximum a posteriori to improve sorting speed and accuracy.

This work builds upon our previous results to develop a low sorting latency and high throughput spike sorting unit on a field programmable gate array (FPGA), assisted by a desktop computer. Our FPGA has the capability to perform real-time spike sorting by matching cluster templates pre-calculated by the desktop computer with neural spikes collected during a short training period. In order to ensure proper template generation, the templates were generated by a desktop computer using a more sophisticated neural spike sorting algorithm—SPC. The cluster templates were then transferred to the FPGA module for subsequent real-time spike sorting through matching the incoming neural spikes to these cluster templates. In order to allow the FPGA to achieve optimal sorting accuracy under different noisy conditions, two template matching methods—Euclidean distance (ED) and correlational matching (CM)—were also implemented in the FPGA and the two methods are selectable by investigators to achieve optimal sorting accuracy according to the type of noise during experiments. Rigorous testing determined that ED yield slightly better sorting accuracy when the spikes are contaminated by Gaussian noise. CM, on the other hand, can handle spike amplitude fluctuations caused by the metal electrode slowly drifting away from its initial implanted

Continuous 

Low-latency single channel real-time neural spike sorting system based on template matching

Pan Ke Wang, Sio Hang Pun, Chang Hao Chen, Elizabeth A. McCullagh, Achim Klug, Anan Li, Mang I. Vai, Peng Un Mak, Tim C. Lei

position within the brain better, such as in long-term (minutes to hours) behavioral neuroscience studies performed on awake behaving animals. The algorithm was also compared with several off-line spike sorting algorithms indicating that the template matching technique achieves comparable sorting accuracies but has a three order-of-magnitude shorter sorting time.

With our approach, a maximal spike sorting rate of 941 spikes/second was achieved for a single electrode. This sorting rate is several times higher than the typical firing rates of neurons, preventing accidental loss of neural spikes in the sorting. The sorting latency of processing a neural spike was measured to be less than 2 ms, which should be fast enough to be used to analyze neural spike data in closed-loop neural control settings. The sorting rate and latency are approaching the theoretical limits set since the natural spike width of an action potential is ~ 1 ms, making the theoretical maximum sorting rate ~ 1000 spikes/second for a single electrode. In addition, the FPGA can also handle a maximum of eight neural clusters, which is generally more than the number of neurons a middle to high impedance metal electrode can simultaneously record.

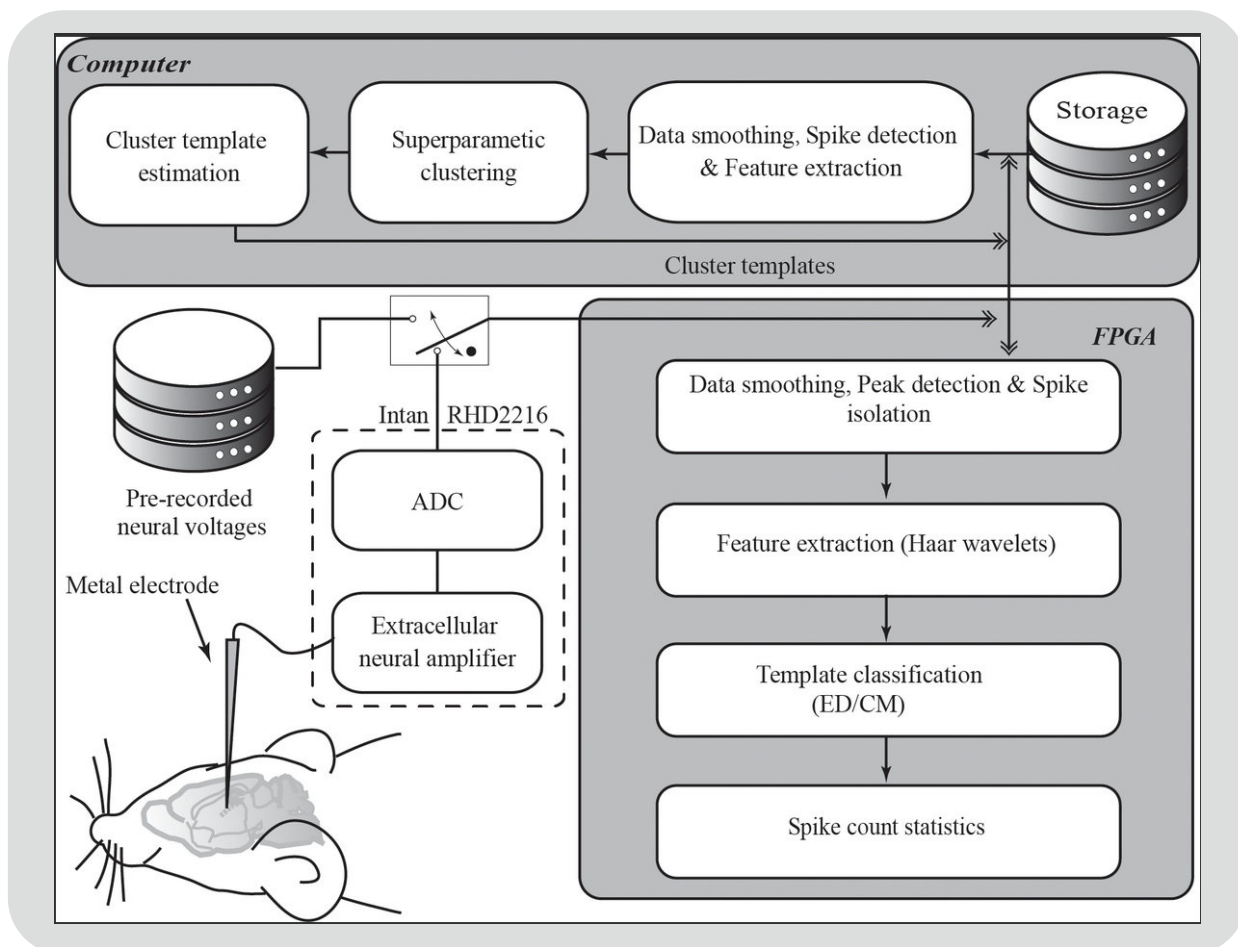


Figure 1 Block diagram of the real-time spike sorting system.

The system is comprised of a desktop computer and an FPGA module. The system can measure extracellular neural spikes from an animal with a neural amplifier and an analog-to-digital converter (ADC), or alternatively be directly injected with digitized pre-recorded neural voltages for system testing. The desktop computer contains three sub-processing units– 1) raw data smoothing, spike detection and feature extraction, 2) spike sorting using SPC and 3) template estimation. The FPGA module also contains four sub-processing units– 1) raw data smoothing, peak detection and spike isolation, 2) feature extraction, 3) neural spike sorting based on template matching, and 4) calculation of spike count statistics.

Continuous

Low-latency single channel real-time neural spike sorting system based on template matching

Pan Ke Wang, Sio Hang Pun, Chang Hao Chen, Elizabeth A. McCullagh, Achim Klug, Anan Li, Mang I. Vai, Peng Un Mak, Tim C. Lei

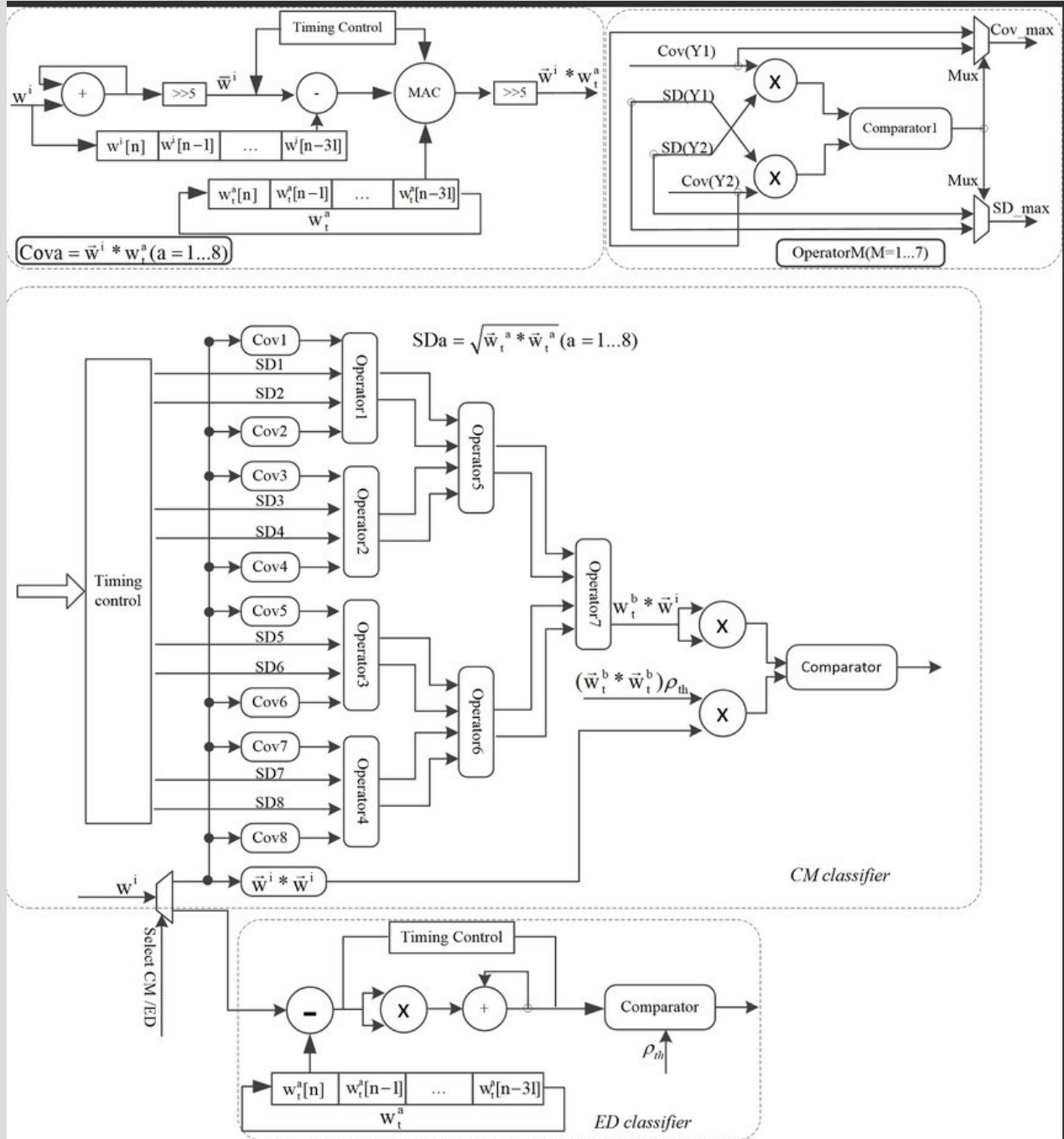


Figure 2 Hardware implementation of the CM and ED classifiers. Investigators can select one of the two classifiers through the “Select CM/ED” pin. Within the CM classifier, there are in total 8 covariance units (Cova) and 7 operator units (OperatorM) for determining the maximum correlation coefficient for the incoming spike to the eight cluster templates. Based on this design, the covariance calculations are performed in parallel to achieve minimum calculation latency. The hardware implementation of the covariance units, the operator units, and the ED classifier are also shown in detail on the top two sections and the bottom section of the figure.

Continuous

Low-latency single channel real-time neural spike sorting system based on template matching

Pan Ke Wang, Sio Hang Pun, Chang Hao Chen, Elizabeth A. McCullagh, Achim Klug, Anan Li, Mang I. Vai, Peng Un Mak, Tim C. Lei

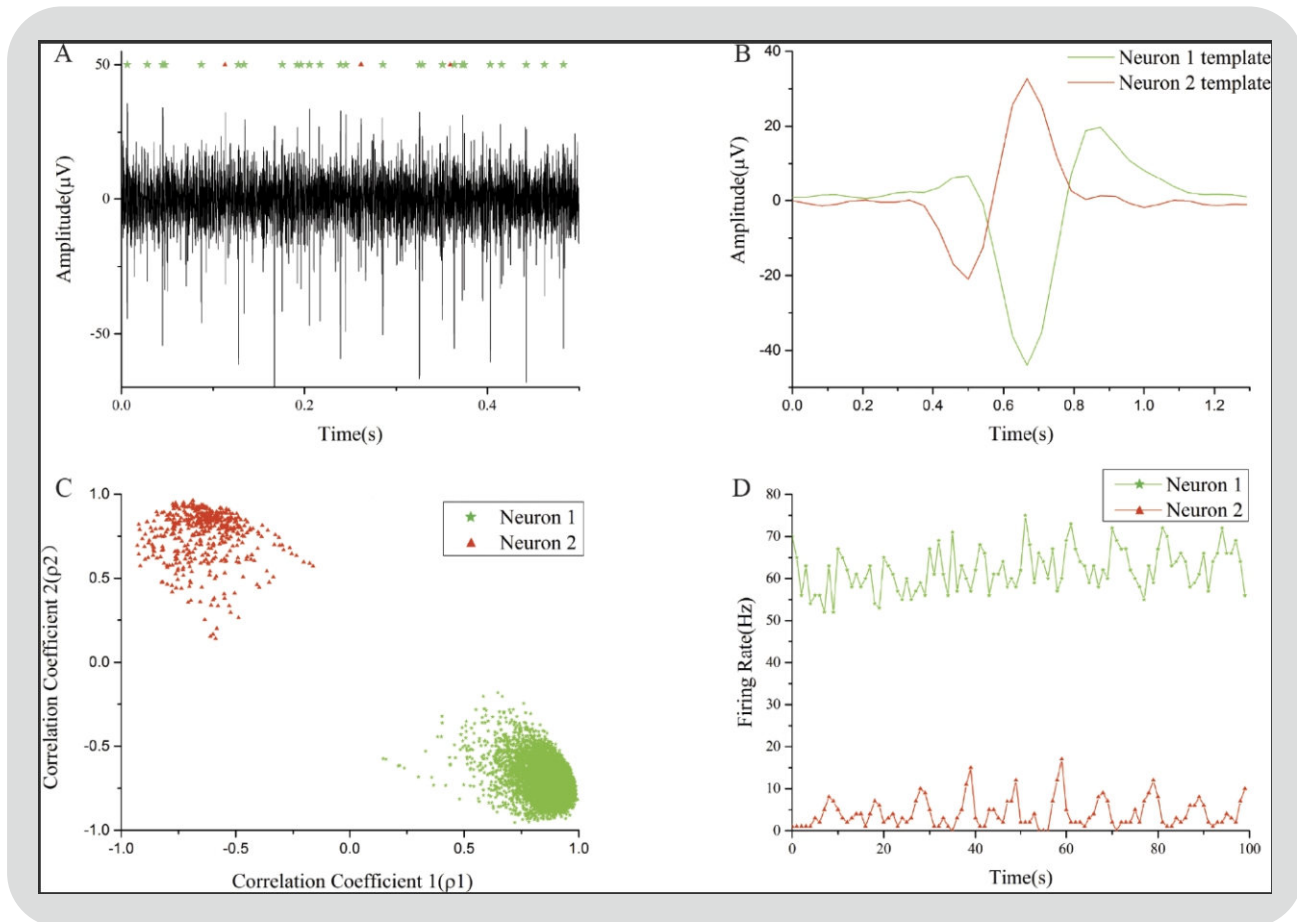


Figure 3 Real-time spike sorting results based on pre-recorded neural spikes from an anesthetized gerbil. (A) 0.5 s of neural voltage trace recorded from the brain stem of an anesthetized gerbil. The green stars and red triangles at the top of the figure indicate the locations of neural spikes of two neurons co-recorded by the same electrode. (B) Temporal profiles of the two cluster templates of the two neurons estimated by SPC. (C) Phase plot of the two cluster groups (green star and red triangle) with each marker representing a neural spike. (D) The firing rates of the two clusters calculated over the 100 seconds of neural data by the FPGA hardware

Publication(s)

Wang PK, Pun SH, Chen CH, McCullagh EA, Klug A, Li A, et al. (2019) Low-latency single channel real-time neural spike sorting system based on template matching. PLoS ONE 14(11): e0225138. <https://doi.org/10.1371/journal.pone.0225138>

Wang, Pan Ke; Chen, Chang Hao; Pun, Sio Hang; Zhang, Baijun; Mak, Peng Un; Vai, Mang I.; Lei, Tim C.: 'Parallel architecture to accelerate superparamagnetic clustering algorithm', Electronics Letters, 2020, 56, (14), p. 701-704, DOI:10.1049/el.2020.0760

Sponsorship

AMSV Research Report 2017–21 Category Here (Please select in the form) Macau Science and Technology Development Fund (FDCT), Research Committee of University of Macau, National Natural Science Foundation of China, National Institutes of Health (NIH) Grant USA